Numerical Study of Wind Excited Action on H Plan-Shaped Tall Building

Ritu Raj[1], Tushar Rana[2], Tushar Anchalia[2] and Utkarsh Khola[2]
[1]*Assistant Professor, Department of Civil Engineering, Delhi Technological University (Delhi), India.*
[2]*UG Student, Department of Civil Engineering, Delhi Technological University (Delhi), India.*

ABSTRACT: Due to the inadequacy of land these days, there is a growing need for tall vertical structures. With this growing need, the plan of the buildings is getting more unconventional as more slender structures are being proposed which makes them highly receptive to wind load. This calls for the analysis of wind load on several structures and the interference response of the structure due to the presence of other structures in its vicinity. This paper is focused on observing variance in the distribution of pressure on different faces of an H plan-shaped tall building model because of the interference effect of a similar plan-shaped tall building of the same height. The computational fluid dynamics program of ANSYS, entitled ANSYS CFX, is utilized for the analysis of the variance of pressures dissemination on the faces of 'H' plan shaped tall building (principal building) due to interference effect for a wind incidence angle of 0°. The buildings are closely spaced (distance is held as 0.1H between the principal building and the interfering building, where H is the building height) and the position of the interfering building is varied with respect to the principal building in three different cases. Various scenarios dependent on varying positions of the interfering building are examined and a comparison is drawn with the 'H' plan-shaped building under wind load at 0° angle of wind incidence in isolated conditions. Pressure contours are plotted for all the surfaces of the 'H' plan shaped building in isolated condition and for different interference cases and the coefficient of pressure (C_{pe}) for all the faces of the building is determined. The flow pattern in the vicinity of the building is also shown to interpret the flow characteristics and vortices generation. Variation of C_{pe} through the horizontal and vertical centerline of the surfaces of the building shows peculiar pressure distribution owing to the interference effect caused by the building in the vicinity of the principal building.

Keywords: ANSYS CFX, computational fluid dynamics (CFD), H plan-shaped tall building, Interference Effect .

I. INTRODUCTION

Wind engineering is characterized primarily as wind interaction with the man-made structures on the Earth's surface. The purpose of wind engineering is to analyze the effect of wind forces on these structures and the potential detriment of the structures. At present times, due to urbanization, the available land area is not expanding while the population is growing at an exponential rate, particularly in urban areas. So, there has been a shift in the shape and size of the buildings from large horizontal structures in the earlier times to tall vertical structures of unconventional and irregular shapes in recent times. Such buildings are considerably lighter and leaner with the innovation in the new building materials and construction techniques. Such tall buildings are particularly susceptible to wind load due to the generation of the base moment under lateral action of wind, hence, the implications of wind loads on these buildings are therefore to be ascertained with a high degree of belief in ensuring their safety. These buildings are typically constructed in lots and their behavior and reactions are contrasting from that of an isolated building. Although abundant information is available in various international codes regarding the responses of traditional plan-shaped structures, for example, IS 875 (Part 3): 1987, but no information regarding irregular plan-shaped structures or interference effects is available in any international codes. Owing to the insufficiency of information in these international codes,

wind action over unconventional plan-shaped structures is burdensome to predict. The variables are building aesthetics, terrain conditions in the vicinity of the building, the relative distance from the principal building to the interfering building, and angle of attack of wind or wind direction. These variables may or may not incite the wind effects in certain regions. These effects or responses due to wind load of unusual or unconventional shaped structures are approximated by ANSYS CFX (analytical) or through Wind Tunnel Test (experimental). ANSYS CFX provides CFD simulation solutions faster with high-performance computing, meaning that engineers and designers can make better choices in the design process of complex-shaped structures sooner.
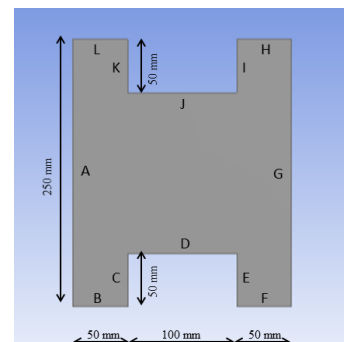
(a)
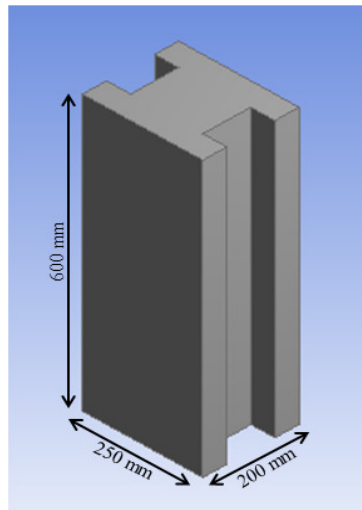
(b)

Fig. 1. Detailed Dimension of the model (a) Plan of H shaped Tall Building, (b) Isometric Plan.

Numerous pieces of literature and researches come up with the study of the effect of wind pressure on high rise buildings and the phenomena of interference between high rise buildings. Franke *et al.,* (2004) provided recommendations for CFD applications in wind engineering ventures based on the statistically steady reproduction of pedestrian wind in built urban areas [1].

Paul and Dalui (2016) studied the wind effects on 'Z' plan-shaped tall building under varying wind directions by CFD and found out the maximum values and directions of extremes of force and pressure coefficients [2]. Mallick *et al.,* (2018) studied the simulation of the wind pressure coefficient on C-shaped building models by means of numerical analysis using ANSYS Fluent and concluded that the pressure on the building was significantly influenced by the structure geometry, orientation, aspect ratios, and wind angle of attack [3]. Abdusemed and Ahuja (2015) did an experimental study on the models of tall buildings with different cross-section shapes (square and triangular) under both isolated and interference conditions. It was concluded that all the components of wind load on triangular-shaped models were larger in value as compared to the square-shaped models and the extremes of all the wind components were determined along with their directions and wind angle [4]. Bhattacharyya *et al.,* (2014) researched about the distribution of pressure on various surfaces of an 'E' plan shaped high rise building under wind angles varying from 0° to 180° and analyzed the model both experimentally (by open-circuit boundary layer wind tunnel) and analytically by CFD in ANSYS CFX. The flow patterns were analyzed for variation of pressure on different faces of the model for various wind angles and variation of pressure along the horizontal and vertical centreline was studied along with pressure variation at different levels [5]. Sheng *et al.,* (2018) investigated the unsteady traits of global and local wind loads and their correlation with the oncoming atmospheric boundary layer via wind tunnel tests on a high-rise building with a well detailed atmospheric boundary at 1:300 scale [6]. Chakraborty *et al.,* (2014) carried out an experimental investigation of surface

pressure on '+' plan tall shaped building in a boundary layer wind tunnel varying the angle of wind incidence from 0° to 45°. Uncanny pressure distributions on certain faces with a severe change in pressure distribution with varying angles were detected [7]. Mukherjee and Bairagi (2017) studied the wind pressure and velocity pattern around 'N' shaped tall buildings. The paper is centered around determining the wind pressure coefficient and wind velocity analysis of the building using k-ε methods [8]. Koliyabandara *et al.*, (2017) analyzed the wind loads on irregular shaped building varying the wind angles at an interval of 45° carrying out the numerical simulation maneuvering Computational Fluid Dynamics (CFD) module Midas NFX [9]. A series of wind tunnel test was carried out in Ankara Wind Tunnel by KURÇ *et al.,* (2012) on a model building which had the shape of a rectangular prism. High-frequency base balance system was employed for data acquisition and effect of wind angle of attack, vortex shedding and turbulence intensity were examined via a sequence of wind tunnel tests [10]. Kheyari and Dalui (2015) investigated the wind loads on a rectangular shaped tall structure under interference effects. The analytical study was carried out by modeling the isolated structure, domain boundaries, and the principal structure with wind angles ranging from 0° to 90°. Downwind structure experiences the most notable interference effects which were dependent upon relative distance, wind angle of attack, and the shape and size of the building [11]. Jana *et al.*, (2015) investigated the empirical analysis of the effects of interference on a pentagonal plan shaped high-rise building and its optimization by adjusting the spacing of two square-shaped buildings and modifying the wind angle of attack [12]. Kar and Dalui (2016) investigated the alteration of pressure at various surfaces of an octagonal plan shaped tall construction due to the interference of the three square plan shaped tall structures of the same height as that of octagonal building. Different cases were contrasted depending on the position of the interfering building with that of an isolated building and interference contours (IF) were analyzed to compare various cases [13].

II. MATERIALS AND METHODS

A. Wind Flow

Design wind pressure. The wind is a natural current of air moving parallel to the ground which is caused by uneven heating of the earth's surface by sun leading to a difference in the atmospheric pressure. The wind moves from a region of high pressure to a region of low pressure. Surface wind is measured by anemometers. Wind speed increases from being zero at ground level to maximum at a height called gradient height. This variation depends on the terrain conditions. If a surface halts wind, the wind's dynamic energy is converted into pressure. The surface-acting pressure transforms into a force called wind-load. The effect of wind load on buildings is therefore calculated to maintain the safety of buildings. Because there is a clear connection between wind load and wind pressure, the design wind pressure is evaluated to ensure the safety of the building. The relation between wind pressure   and wind speed is maneuvered to   evaluate wind pressure at any height above mean sea level:

Pressure $(p_z) = 0.6 * Velocity(V_z)^2$
here,
Pressure(p_z) stands for the pressure of wind in N/m^2 at a height z and Velocity(V_z) refers to design wind speed in m/s at a height z above the mean level.
The design wind pressure p_d can be obtained as:
$p_d = X_d*X_a*X_c*$ Pressure(p_z)
here,
X_d stands for Wind directionality factor, X_a stands for Area averaging factor, and X_c stands for Combination factor

Design Wind Speed. Design wind speed, Velocity (V_z) at any elevation z is adjusted to include consequences due to risk level, the roughness of the terrain, local topography, and factor of importance for the cyclonic area. It is mathematically expressed as:
Velocity $(V_z) = V_b.a_1.a_2.a_3.a_4$
Here,
Velocity(V_z) stands for design wind speed at elevation z (m/s), V_b stands for basic wind speed, a_1 stands for probability factor (risk coefficient), a_2 stands for terrain roughness and height factor, a_3 stands for topography factor, a_4 stands for importance factor for the cyclonic region.

Mean wind speed. Mean wind speed is the speed averaged over a specific time interval with time interval varying from few seconds to few minutes. With the help of the following two models, the mean wind speed with elevation can be presented as:

Logarithmic Law.
$$\frac{V}{V^*} = \log_e\frac{z}{z_o}$$
Here,
k = 0.40(Von Karman's constant),
z = elevation above the surface,
z_o = surface roughness parameter,
And V^* = friction viscosity

Power Law.
$$\frac{V}{V_O} = \frac{z}{z_o}\cdot\alpha$$
here,
V = Velocity at elevation z above the surface,
V_o = Wind speed at reference height,
z_o = Reference height above the surface,
α = the exponent power law which varies for different terrains.
In our study of numerical analysis of wind excited action, Power Law has been practiced from the above two laws for wind associated calculations.

B. Computational Fluid Dynamics
Computational Fluid Dynamics (CFD) is a computerized simulation software that is used to foresee the reverberation of fluid flow around the model by devising a virtual wind tunnel around the model. With the advancement in computing power with the help of high-end graphical processing units (GPU(s)), the CFD technique is a robust accretion of the physical wind tunnel that empowers us to decipher compound wind dilemmas. CFD is a robust technique that enables us to decipher predicaments linked with wind loads on buildings, the interplay of different forces on the structure, and pressures on buildings, etc. CFD is comprised of a handful of methods for calculating the wind flow pattern and model behaviors under the wind effect. In our study, we have used ANSYS 2019-R2 and

within ANSYS we have utilized CFX package of ANSYS with k-ε turbulence modeling to maintain ample resemblance between numerical and experimental techniques.
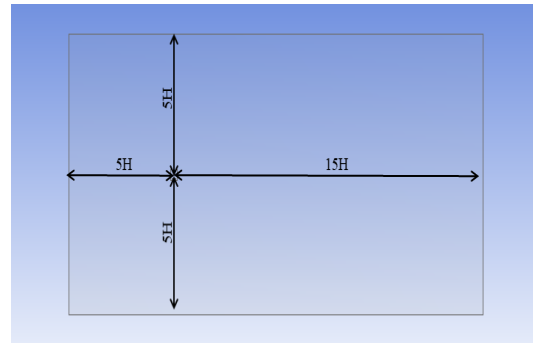
(a)
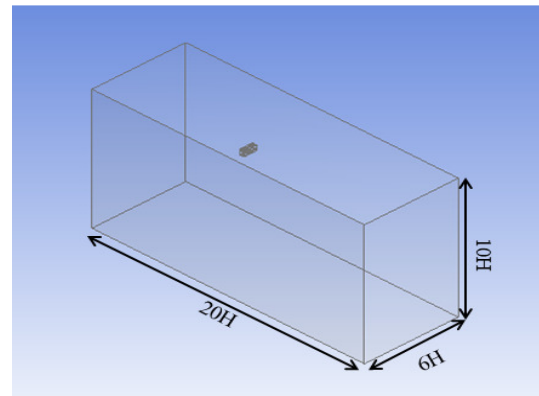
(b)

Fig. 2. Detailed dimension of the domain.

Validation of CFD. Using ANSYS CFX under uniform wind flow, wind loads on isolated square-shaped high-rise buildings for wind angles 0° and 90° are analyzed by k-ε turbulence modeling to validate the pressure coefficients at various faces of the buildings with AS/NZS 1170.2: (2002), BS: 6399-2(1997), EN: 1991-1-4(2005) and IS-875 (part 2) (1987) [8]. The square plan shaped building has a height(H) of 600mm and width(w) of 200mm, so the aspect ratio is 3 (H/w = 3) and 1 (l/w = 1). Uniform wind velocity of 10m/s is provided at the inlet of the domain and the domain configuration is kept the same as suggested by Revuz *et al.,* (2012) [14]. Table 1 depicts the relative comparison between CFD simulation and various codes. The windward face A has a positive pressure while the side faces (B and C) are experienced with negative pressures due to side wash and flow separation. The leeward face D depicts a complete suction (negative pressure). The values of CFD simulation shown in Table 1 validates the values of various codes as shown in the table.

C. Overview of the Model
The dimensions of the model considered in the study are shown in Fig. 1. The principal building and the interfering building are identical in cross-section with a fixed height of 600mm and the buildings are modeled in 1:100 scale. The distance between the buildings is taken as 0.1H which is equal to 60mm. The orientation of the interfering building is changed with respect to the

principal building at an interval of 125 mm. The model was initially exposed to a wind velocity of 10 m/s at an angle of 0° in isolated condition and then interference study is carried out for the wind incidence angle of 0° for three different cases.

The domain configuration adopted for the study was such that the wind response of both the buildings is equivalent to open environment conditions. Also, the domain size was such that the velocity fluctuations, vortex generation, etc. in the wake region are conformed [14]. The inlet and the two-side face of the domain were kept at a distance of 5H from the principal building faces. The outlet of the domain was kept a distance of 15H from the leeward side of the principal building where H is the building's height. The top of the domain had a clearance of 5H from the top of the buildings. Such substantial domain dimensions are sufficient for creating vortex on the leeward side of the building and preventing wind backflow. Fig. 2 shows the domain cross-section.

Finer hexagonal meshing with aid of inflation was adopted in the near vicinity and on the surfaces of the buildings to mimic the steady flow and precisely evaluate the actual behavior of responses. For the remainder of the domain, uniform coarser tetrahedron meshing is adopted to minimize the computation time without any major loss of fidelity. Meshing is depicted in Fig. 3. The boundary walls are considered "FREE SLIP WALLS" except the wall on which the building is resting which is taken as "NO-SLIP WALLS" and the walls of the building are considered "NO-SLIP WALLS".
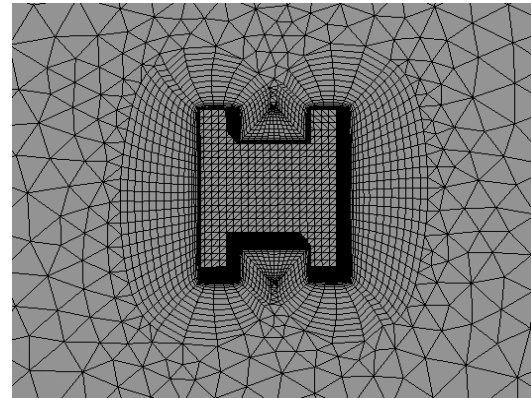
(a)
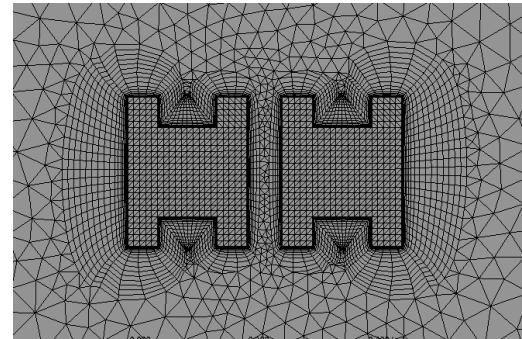
(b)

Fig. 3. The pattern of mesh around (a) the isolated building, and (b) the principal building.

Table 1: Comparative analysis between various codes of provision and CFD simulation for square plan-shape building.

Faces	CFD Simulation		AS/NZS 1170.2: 2002		ASCE 7-02. (2002)		BS: 6399-2 (1997)		EN: 1991-1-4 (2005)		IS-875 (part 3) 1987	
	0°	90°	0°	90°	0°	90°	0°	90°	0°	90°	0°	90°
Windward	0.85	0.85	0.80	0.80	0.80	0.80	0.85	0.85	0.80	0.80	0.80	0.80
Leeward	-0.46	-0.46	-0.50	-0.50	-0.50	-0.50	-0.50	-0.50	-0.63	-0.63	-0.25	-0.25
Side face	-0.71	-0.71	-0.65	-0.65	-0.70	-0.70	-0.80	-0.80	-0.80	-0.80	-0.80	-0.80

III. RESULTS AND DISCUSSION

The results obtained in the study are discussed in this section. ANSYS CFX is utilized to compute C_{pe}, the external pressure coefficient, using the formula:
$$C_{pe} = P / (0.6 * V_z^2)$$
Where P is the surface pressure and V_z is the design speed. A positive pressure coefficient implies that the surface has a positive pressure and wind is directly dissipated at the surface while a negative pressure implies suction pressure due to vortices generation and flow separation. The following sections show a detailed comparative study of isolated and interfering conditions.

A. Isolated Condition

This section elaborates on the results obtained on an isolated H plan-shaped building for wind incidence angle 0°. The pattern of wind flow around the building is depicted in Fig. 9 (a). From the flow patterns, the flow traits, eddies generation, and vortices are evidently discernible. The variation of wind pressure for individual faces of the buildings is shown in Fig. 5. Positive pressure occurs on the windward sides of the building because of head-on wind collision with the surface and

negative values occur at the leeward side of the building due to pressure suction. The average face values of the external pressure coefficient, C_{pe} of the isolated building for wind angle 0° is shown in Table 2 of the interference factor. The variation of C_{pe} along a vertical centerline for different faces of the isolated building is shown in Fig. 10. Referring to Fig. 10(a), for wind angle 0°, it is quite obvious that Face A, being the windward face has positive pressure while the edges of Face A has a negative pressure due to wind deflection and flow separation around edges of Face A. Face A has the highest average C_{pe} due to direct wind impact. Due to the symmetry of the building, the building experiences symmetrical pressure distribution on different faces. Side faces B and L show identical non-uniform pressure distribution due to side wash and vortices formation which leads to a high negative value of C_{pe}. Face C and Face K also exhibits identical non-uniform pressure distribution. Face D and Face J are identical and are in complete suction due to vortices formation Face E and Face I show an almost uniform pressure distribution up to a definite height and subsequently the pressure increases towards the top of the building. Face F and

Face H are also in suction and depicts the non-uniform distribution of pressure. Vortices are formed around the leeward face (Face G) of the building which leads to pressure suction and non-uniform pressure variation along the face. The pressure first increases then decreases drastically and then again increases. Face A shows the maximum pressure because of undeviating wind dissipation while Face B shows maximum suction due to side wash and vortices generation.

B. Interfering Condition

In this scenario, the buildings are subjugated to wind angle of 0° only with boundary layer wind flow. The orientation of the interfering building, however, is changed with respect to the principal building, with a full blockage in the first case, partial blockage in the second case, and total clearance in the third. Simplified plan illustration of the principal, as well as the interfering building, is shown in Fig. 4. The distance between the two buildings is kept constant at 60 mm (0.1H).

Case 1. 'y' = 0 mm

In case of complete blockage by interfering building, the principal building experiences complete suction. The wind flow pattern around the buildings is shown in Fig. 9(b).
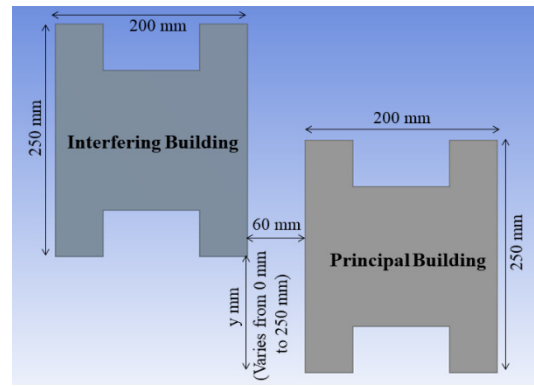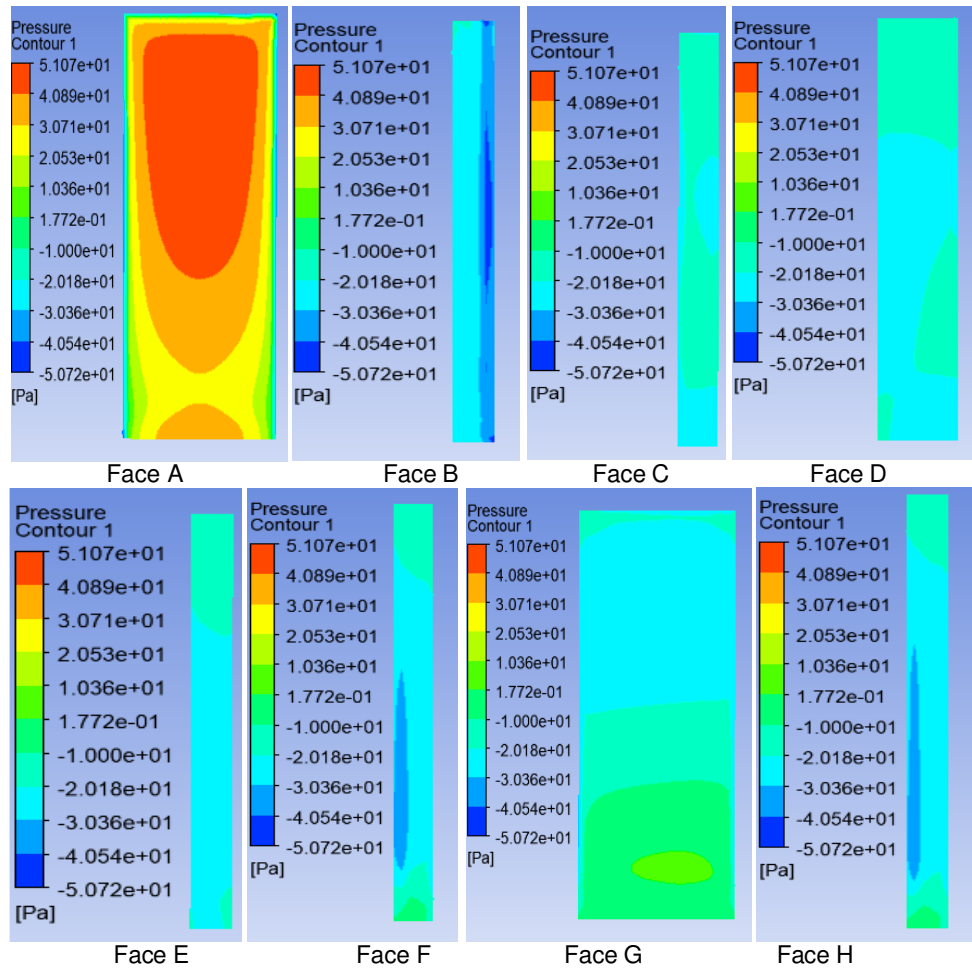

Fig. 4. Simplified plan illustration of H plan-shaped tall building under wind incidence angle of 0°.

One can see the points of vortex generation in the figure. Vortices are established around the principal building which leads to the build-up of negative pressure around the principal building.
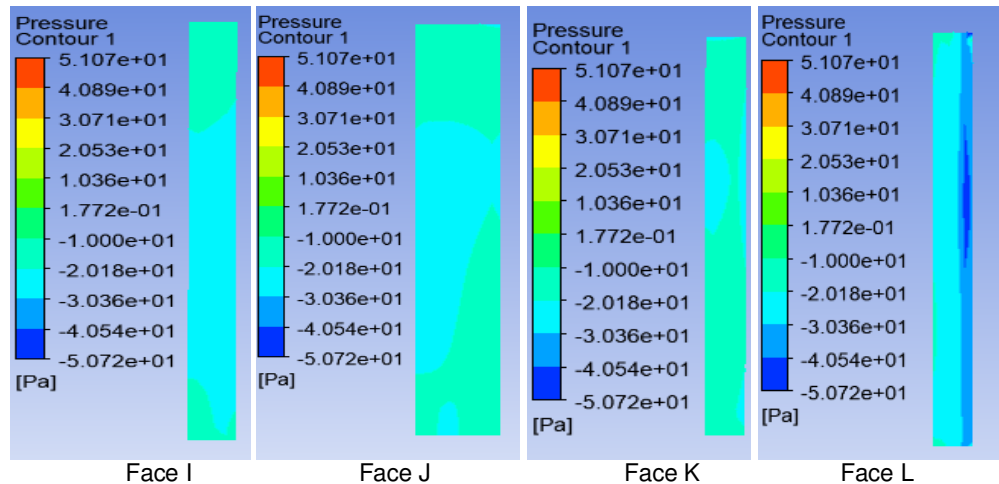

Face A   Face B   Face C   Face D

Face E   Face F   Face G   Face H

Fig. 5. Pressure contours (wind pressure variation) for 0° wind angle on different faces of an H-shaped tall building around the principal building.

Pressure contours of all the principal building faces are displayed in Fig. 6. The variation of C_{pe} through the vertical centerline of the faces is shown in Fig. 10. Face A shows negative uniform pressure due to the generation of vortices and pressure suction. Face B and Face L shows identical pressure contours and pressure variation due to the symmetry of the model. The pressure variation is non-uniform in both cases. Face C and Face K depicts alike behavior showing a non-uniform variation of pressure. Face D and Face J are identical and depict consistent pressure up to a definite height. Face E and Face I first experiences a pressure decrease followed by a uniform pressure till a specific height and then finally the pressure increases. Face F and Face H shows a parabolic variation of pressure distribution. Face G shows nearly constant pressure till a specific height after which the pressure decreases. Fig. 11 displays a contrast of pressure differences through the horizontal centerline line (horizontal line along the perimeter of the building at H/2) for an isolated building and the principal building under interference effect (case 1). In the case of an isolated building, Face A experiences a direct wind incidence, and hence the pressure reaches a maximum at the center of the face and drops to negative values around the periphery due to side wash and separation of flow. However, in the case of the principal building, Face A experiences pressure suction and hence negative values of C_{pe} are obtained due to vortices generation. There is a common belief that wind loads are less severe in a building when surrounded by other structures than in an isolated building. In this case, however, the pressure on all sides of the main building except face A is higher than the pressure on the isolated building.

Case 2. 'y' = 125 mm
In this scenario, the interfering building partly blocks the movement of the wind to the principal building. The distance between the buildings is kept constant at 60mm while the distance between 'y' is increased from 0 to 125mm. Variation of the pressure distribution of all the faces and the dissimilitude of C_{pe} along the vertical centerline of the faces is shown in Fig. 7 and Fig. 10 respectively. In this case, Face A shows a positive pressure towards the right side of the building due to

direct wind impact. However, a major portion of the face is still in suction due to vortices generation and hence a very small value of C_{pe} is obtained. Suction pressure is seen on Face B due to side wash. Face C, Face D, and Face K show a non-uniform variation of pressure, and pressure keeps on decreasing with height. Face E exhibits a decrease of pressure up to a certain height after which the pressure increases and becomes positive towards the top of the face. Face F, Face G, and Face H shows a non-uniform variation of pressure. In the case of Face I and Face L, the pressure first increases up to a certain height and decreases afterward.

Referring to Fig. 12, the pressure on Face A of the principal building increases towards the right reaches a maximum and then decreases towards the edges due to flow separation. Face A of isolated building experiences more pressure than that of the principal building due to direct wind incidence. The pressure variation on Faces B, C, D, E, and F are quite similar both the cases with pressure on the principal building being slightly higher. However, Face G of the isolated building experiences more pressure than Face G of the principal building which is caused by the vortices generation around Face G of the principal building. The curve is less or more constant in the case of the principal building. In both cases, maximum suction occurs at Face B.

Case 3. 'y' = 250 mm
In this scenario, the interfering building is in the vicinity of the principal building and the value of 'y' is increased from 125mm to 250mm so there is no portion of the interfering building in front of the principal building. Variation of the pressure distribution of all the faces and the dissimilitude of Cpe through the vertical centerline of the faces is shown in Fig. 8 and Fig. 10 respectively There is a direct impact of wind on the principal building. Face A of the principal building exhibits a positive pressure similar to the isolated condition due to direct wind dissipation. The variation of pressure is also similar to that of the isolated building. There is suction around the edges of Face A. In the case of Face B, the pressure decreases up to a certain height and then goes on increasing. The pressure on Face B in more than the previous case (case 2) due to the less

interference. The pressure remains almost constant in case of Face C, Face D, Face E, Face I, Face J, and Face K of the principal building.

Referring to Fig. 13, pressure variation on Face A of both the principal and the isolated buildings is similar due to the direct incidence of wind. The pressure of Face A of the isolated building is slightly higher than that of the principal building as there is no interference in the case of an isolated building. Suction near face B, face C, face D, face E, and face F of the principal building due to flow separation from the isolated and the principal buildings due to which these faces of principal

building experience reduced pressure as compared to the isolated building. Face F of the isolated building shows a positive pressure towards the center of the face, however, no such trend is seen in the case of the principal building. Face G of the principal building has a higher pressure than that of the isolated building. Rest all faces of both the principal and the isolated building experience suction with the pressure on the faces of the isolated building being slightly higher.
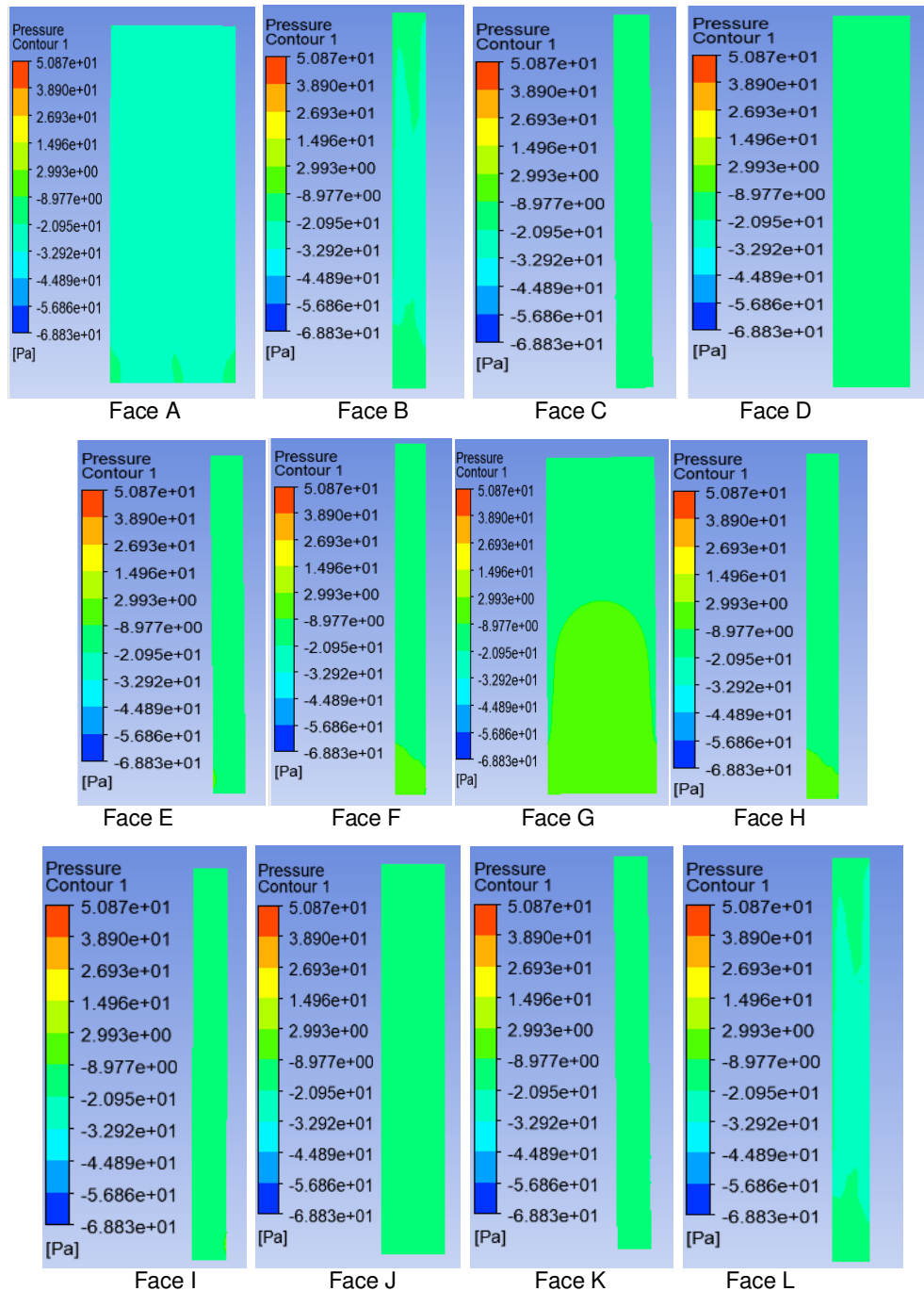

Fig. 6. Pressure contours (wind pressure variation) for 0° wind angle on different faces of an H-shaped tall building under case 1.
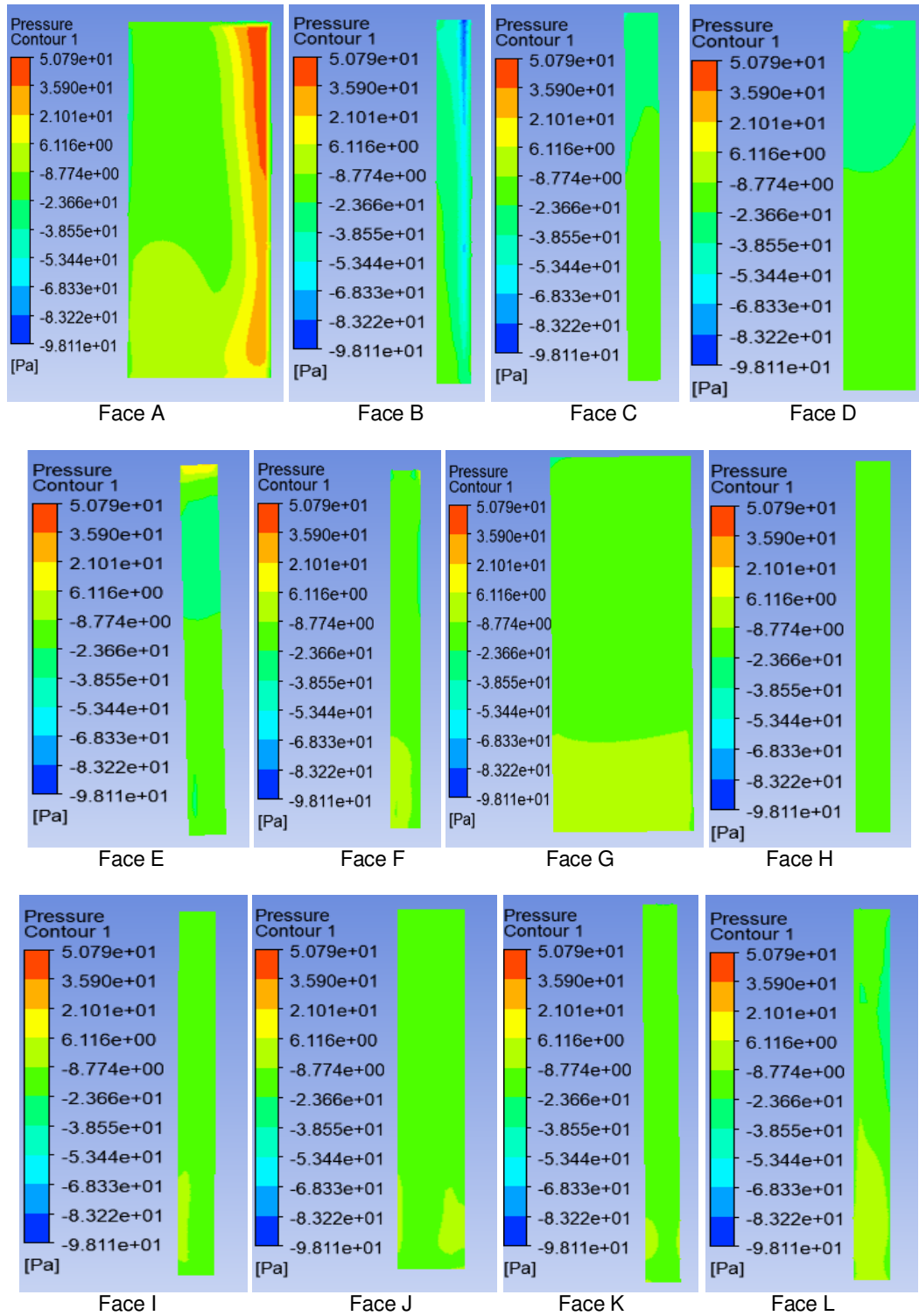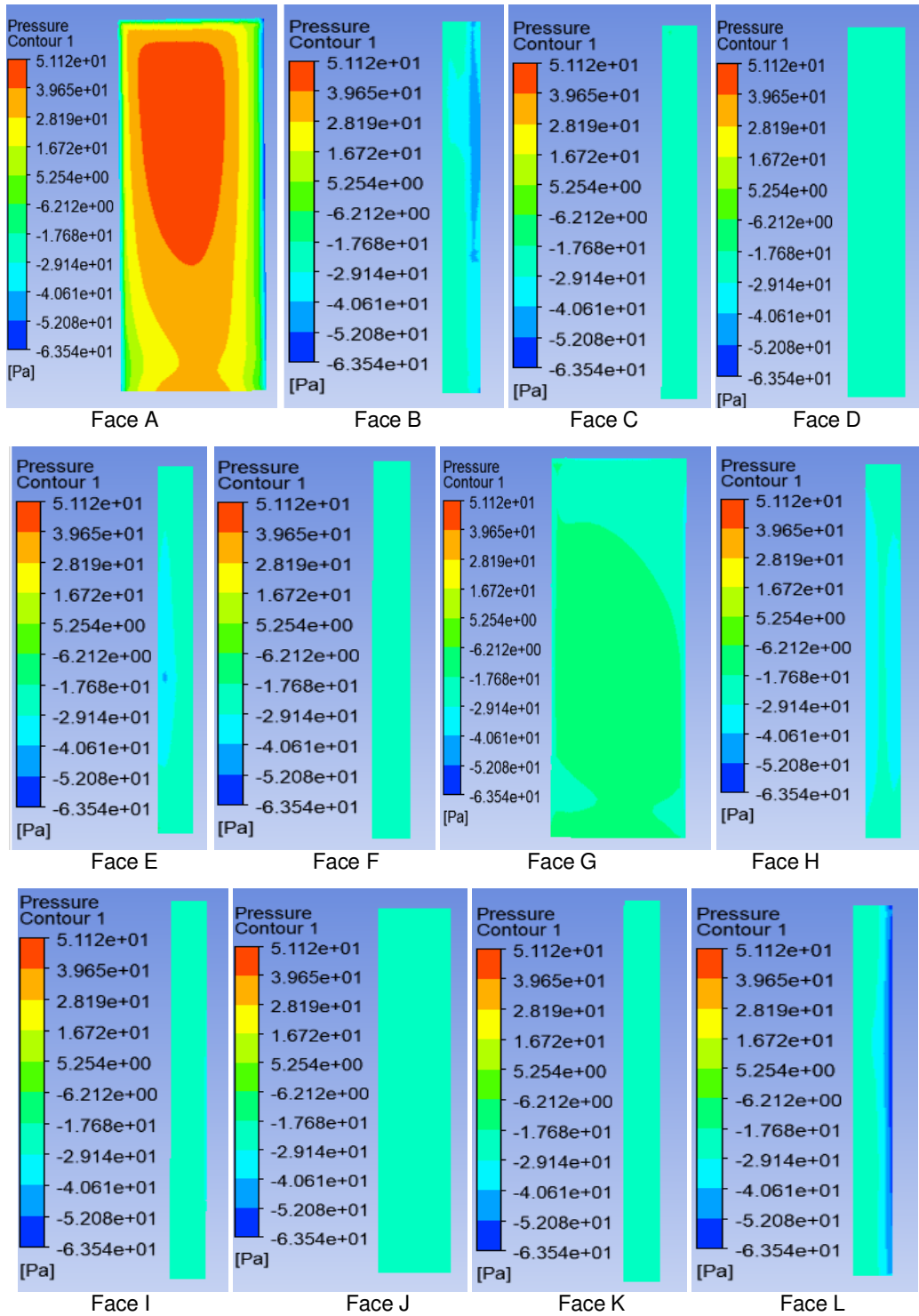
Fig. 7. Pressure contours (wind pressure variation) for 0° wind angle on different faces of an H-shaped tall building under case 2.

Fig. 8. Pressure contours (wind pressure variation) for 0° wind angle on different faces of an H-shaped tall building under case 3.
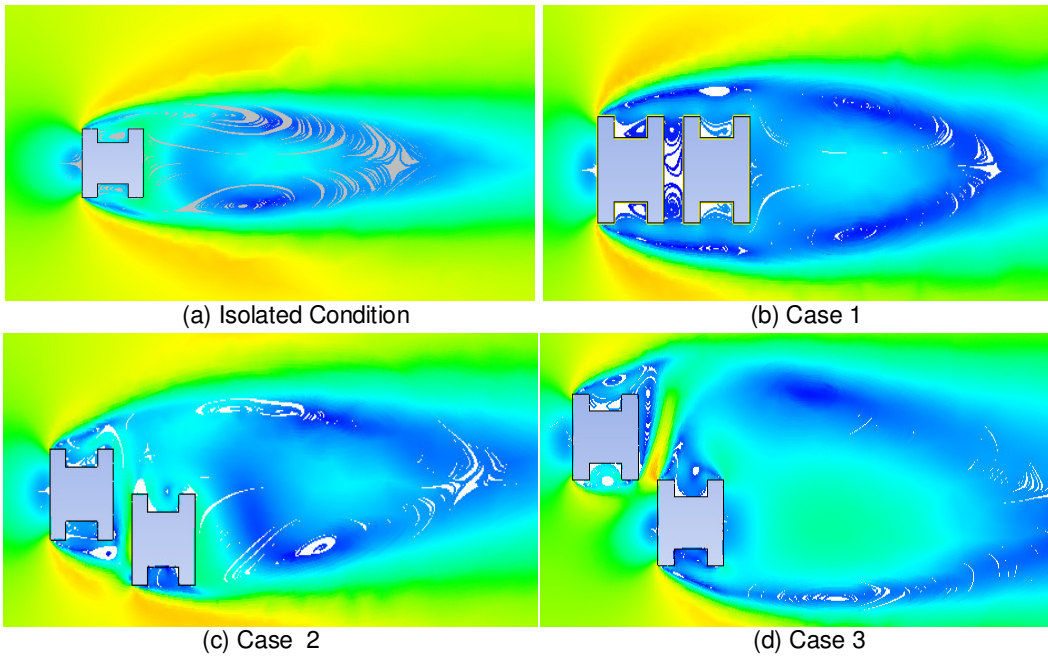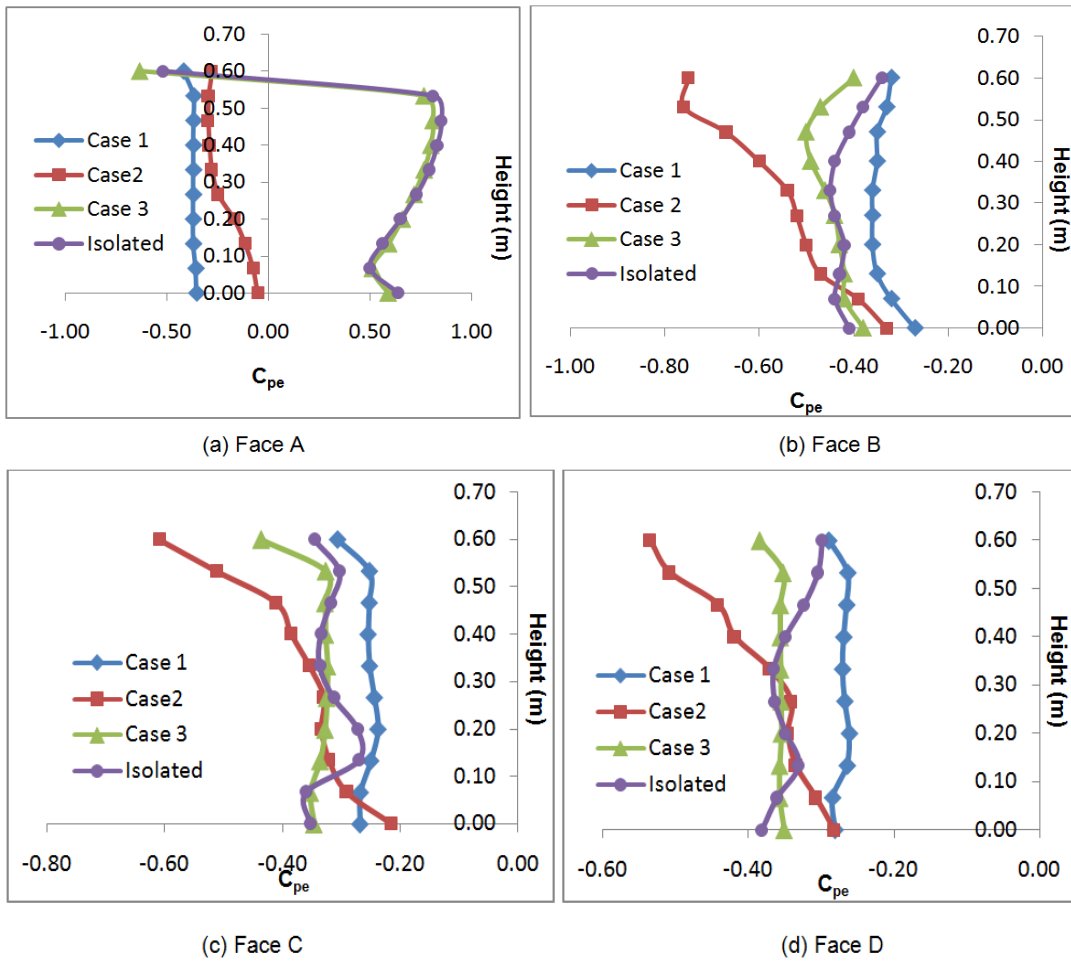
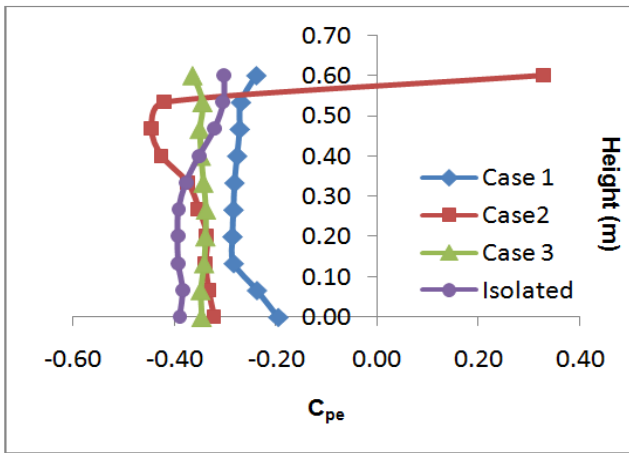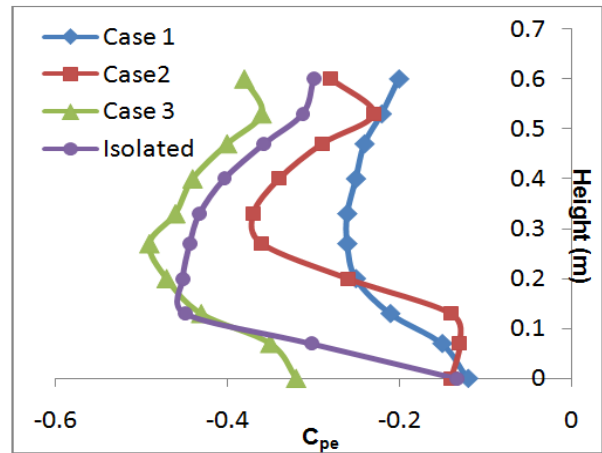(a) Isolated Condition   (b) Case 1

(c) Case 2   (d) Case 3

Fig. 9 Pattern of Wind Flow in the vicinity of (a) the isolated building and ((b), (c), (d)) the principal building under different cases.

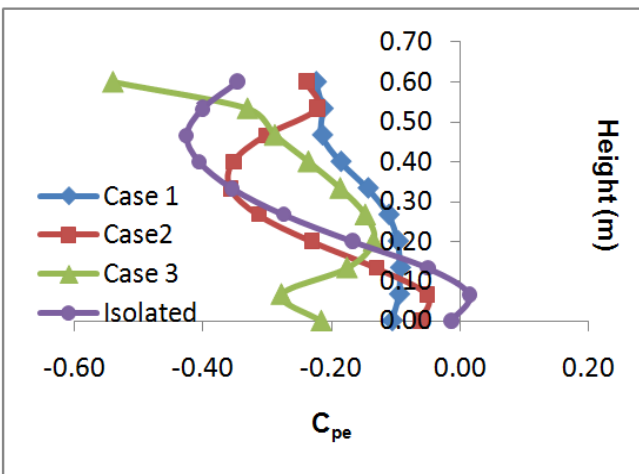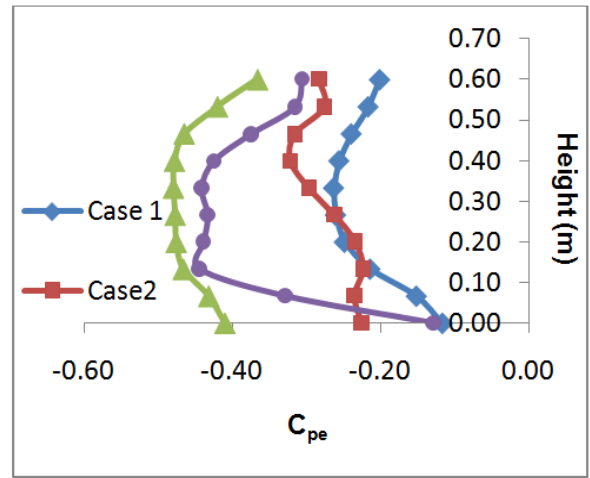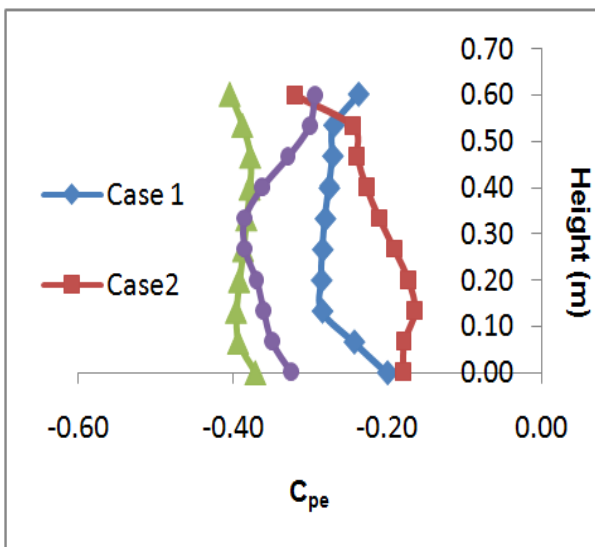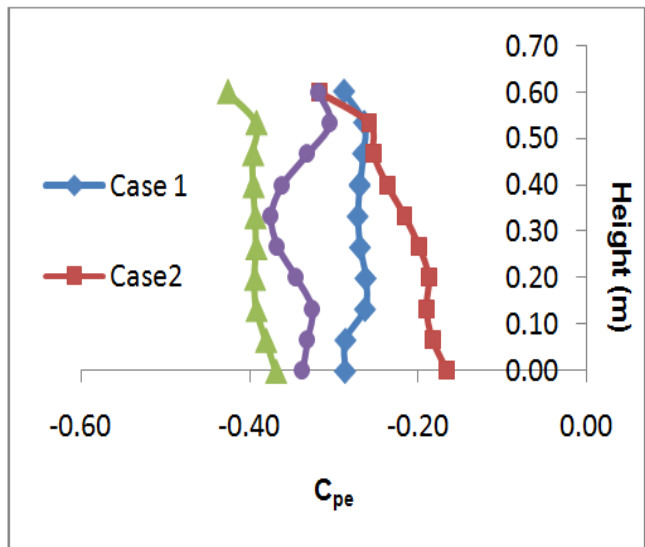(a) Face A   (b) Face B

(c) Face C   (d) Face D

(e) Face E

(f) Face F

(g) Face G

(h) Face H

(i) Face I

(j) Face J

(k) Face K

(l) Face L

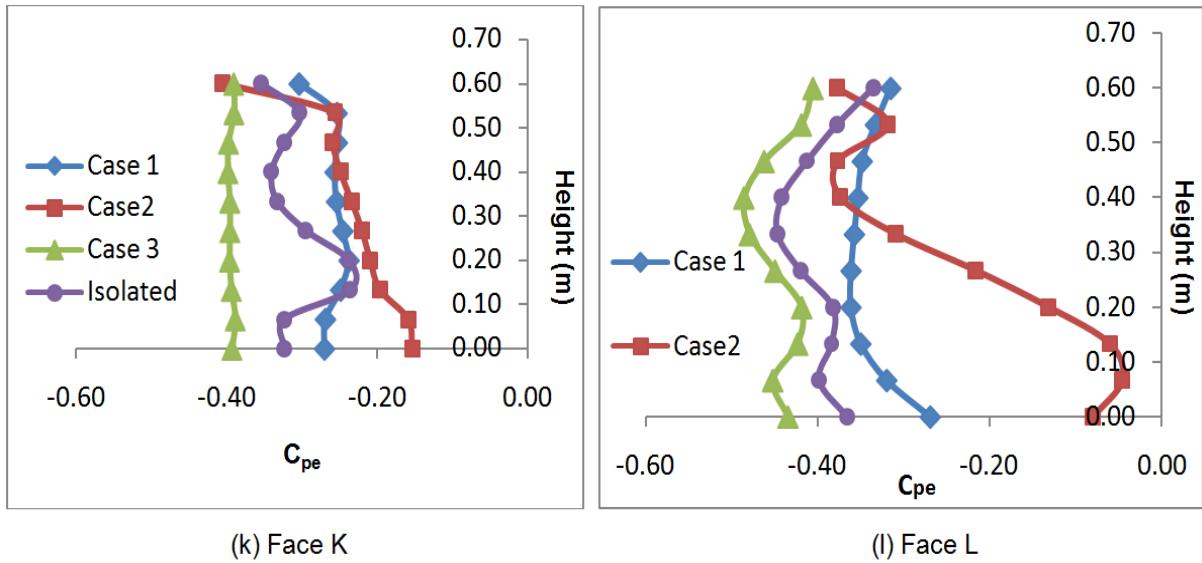**Fig. 10.** Variation of C_{pe} (pressure coefficient) through the vertical centerline of all the surfaces the principal building.
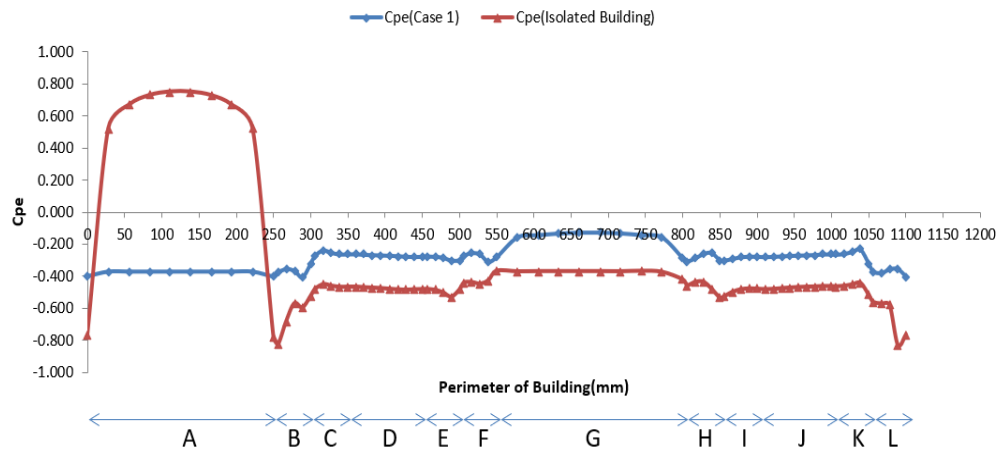

Fig. 11. Pressure coefficient variation along the horizontal centerline for principal building and isolated building (Case 1)
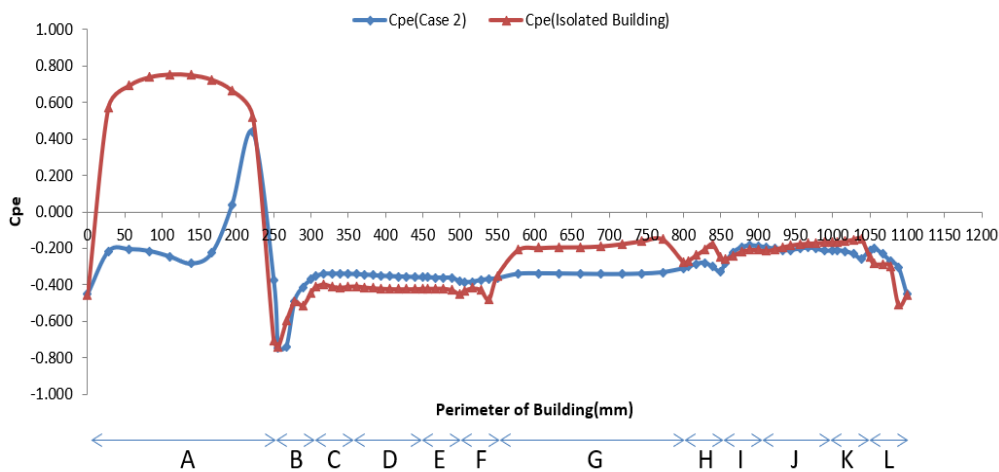

Fig. 12. Pressure coefficient variation along the horizontal centerline for principal building and isolated building (Case 2).
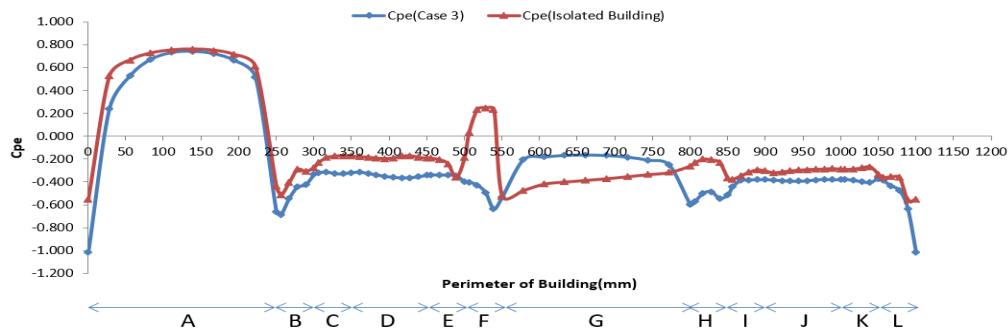
Fig. 13. Pressure coefficient variation along the horizontal centerline for principal building and isolated building (Case 3).

Interference Factor (IF): The effects of the interference are described as non-dimensional interference factors (IFs) [11] reflecting aerodynamic forces on the H-shaped structure, with interference from a close-by similar shaped building plan. IF is, therefore, a multiplier factor utilized to evaluate wind pressure on a building with interference effects. IF varies depending on structural orientation, aspect ratio, state of the topography, location of the structure interfering, etc. The formula for IF is described as:

$$I.F. = \frac{\text{Average wind pressure on the surface of the principal building under interference effect}}{\text{Average wind pressure on the face of the isolated building under no interference condition}}$$

Table 2: Interference Factor.

	Faces	C_{pe} (Isolated Building)	C_{pe} (Principal Building)	Interference Factor
Case 1	A	0.491	-0.374	-0.761
	B	-0.489	-0.348	0.712
	C	-0.327	-0.263	0.806
	D	-0.340	-0.263	0.772
	E	-0.367	-0.267	0.729
	F	-0.394	-0.232	0.590
	G	-0.268	-0.160	0.597
	H	-0.395	-0.235	0.594
	I	-0.355	-0.268	0.756
	J	-0.332	-0.263	0.793
	K	-0.309	-0.264	0.853
	L	-0.464	-0.349	0.751
Case 2	A	0.491	-0.079	-0.160
	B	-0.489	-0.581	1.187
	C	-0.327	-0.384	1.173
	D	-0.340	-0.376	1.105
	E	-0.367	-0.343	0.935
	F	-0.394	-0.271	0.687
	G	-0.268	-0.234	0.874
	H	-0.395	-0.284	0.719
	I	-0.355	-0.222	0.625
	J	-0.332	-0.206	0.621
	K	-0.309	-0.222	0.718
	L	-0.464	-0.259	0.558
Case 3	A	0.491	0.396	0.806
	B	-0.489	-0.506	1.035
	C	-0.327	-0.337	1.030
	D	-0.340	-0.348	1.025
	E	-0.367	-0.352	0.959
	F	-0.394	-0.426	1.082
	G	-0.268	-0.276	1.032
	H	-0.395	-0.495	1.253
	I	-0.355	-0.399	1.123
	J	-0.332	-0.384	1.155
	K	-0.309	-0.384	1.243
	L	-0.464	-0.539	1.162

Table 2 shows IF values corresponding to different facets of the main building in three different cases. In case 1, it is observed that all facets of the isolated building except face A, have higher suction values than the facets of the main building. In case 2, Face B, C and D of the principal building have higher suction values owing to the separation of flow and vortices generation, and hence IF values for these respective faces are greater than 1. Only Face A of the main building experiences positive pressure in case 3, but it is less than that of an isolated building, therefore IF value less than 1 is obtained. The suction values of all the faces except that of Face E of the main building are greater than the isolated building which is caused by flow separation and vortices. Hence, IF values greater than 1 are obtained.

IV. CONCLUSION AND FUTURE WORK

The conclusions drawn from the study are presented in this section. So far, there is no provincial code providing specific details on wind loads on irregular plan-shaped construction and the interference effects induced by the presence of other structures in the vicinity of the main structure. This study focused on the wind loads induced on the surfaces of H plan-shaped tall building under isolated conditions for wind incident angle of 0° and interference effects induced by the similar plan-shaped tall building on the principal H plan-shaped building. The important findings of this analysis on H plan-shaped tall building are summed up as:

– In isolated conditions at 0° wind incidence angle, the H plan shaped building experience symmetrical pressure distribution. Positive pressure occurs on the windward sides of the building due to un-deviated wind impact and negative values occur at the leeward side of the building due to pressure suction Face A shows the maximum pressure due to direct wind dissipation while maximum suction occurs on Face B of the isolated building due to side wash and vortices formation.

– In case 1, where the value of 'y' is zero, the interfering building completely blocks the wind flow to the principal building, the pressure on all faces of the principal building except Face A is greater than the pressure on the isolated building which is opposite to what was anticipated.

This is due to the fewer gaps i.e. 60mm between the isolated and the principal building during CFD simulation and the interference effect caused by the adjacent building.

– In case 2, where the value of 'y' is increased to 125 mm, interfering building partly blocks the wind flow to the principal building. Face A of the principal building shows positive pressure along with suction with the point of maximum pressure shifting towards the right due to the flow separation by the interfering building. Face G of the isolated building experience more pressure than Face G of the principal building which is caused by the vortices generation around Face G of the principal building. Maximum suction exists on Face B of both the principal and isolated buildings.

– In case 3, where the value of 'y' is increased to 250 mm, the interfering building does not block the direct incidence of wind on the main building's windward face (Face A), which is why the response of face A is quite

similar in the case of the isolated building and the principal building under interference conditions. However, Face A of the principal building experience slightly less pressure due to the interference effect. The maximum suction point occurs on Face L of the principal building due to vortices generation.

From this analysis, it was found that the principal building has major interference effects and these effects are highly dependent upon the orientation of the building, the relative distance between the buildings, the terrain, and the incidence wind angle. Since a very limited study is carried out in this field, therefore it is imperative to study the proximity effects on the main building with several other buildings of different plans in the vicinity of the main building. The effects of aerodynamics modification like openings, corner modification, etc. on the wind pressure distribution should also be analyzed. The dynamic response analysis of the building using time-varying wind data should also be considered in future studies. Since, very limited information is available in the international codes for the design of complex-shaped structures, the findings of this study would help forecast wind loads on real-life structures for structural engineers and designers.

REFERENCES

[1]. Franke, J., Hirsch, C., Jensen, A. G., Krüs, H. W., Schatzmann, M., Westbury, P. S., & Wright, N. (2004). Recommendations on the use of CFD in predicting pedestrian wind environment. *In Cost action C, 14*, 1-12.

[2]. Paul, R., & Dalui, S. K. (2016). Wind effects on 'Z'plan-shaped tall building: a case study. *International Journal of Advanced Structural Engineering, 8(*3), 319-335.

[3]. Mallick, M., Mohanta, A., Kumar, A., & Raj, V. (2018). Modelling of wind pressure coefficients on C-shaped building models. *Modelling and Simulation in Engineering,* 1-13.

[4]. Abdusemed, M. A., & Ahuja, A. K. (2015) Wind Loads on Triangular Shape Tall Buildings. *International Journal of Engineering and Applied Sciences, 2*(5), 72-75.

[5]. Bhattacharyya, B., Dalui, S. K., & Ahuja, A. K. (2014). Wind Induced Pressure on (E) Plan Shaped Tall Buildings. *Jordan Journal of Civil Engineering, 159*(3267), 1-15.

[6]. Sheng, R., Perret, L., Calmet, I., Demouge, F., & Guilhot, J. (2018). Wind tunnel study of wind effects on a high-rise building at a scale of 1: 300. *Journal of Wind Engineering and Industrial Aerodynamics, 174*, 391-403.

[7]. Chakraborty, S., Dalui, S. K., & Ahuja, A.K. (2014). Experimental Investigation of Surface Pressure on " + " Plan Shape Tall Building. *Jordan J. Civ. Eng., 8*, 251–262.

[8]. Mukherjee, A., & Bairagi, A. K. (2017). Wind pressure and velocity pattern around 'N'plan shape tall building—A case study. *Asian J. Civil Eng., (BHRC), 18*(8), 1241-1258.

[9]. Koliyabandara, N., Jayasundara, H. M. A. D., & Wijesundara, K. K. (2017). 'Analysis of wind load on an irregular shaped tall building using numerical simulation.

[10]. KURÇ, Ö., Kayisoglu, B., Shojaee, S., & UZOL, O. (2012). Investigation of Wind Effects on Tall Buildings through Wind Tunnel Testing.

[11]. Kheyari, P., & Dalui, S. K. (2015). Estimation of wind load on a tall building under interference effects: a case study. *Jordan Journal of Civil Engineering,* 1-18.

[12]. Jana, D., Bhaduri, T., & Dalui, S. K. (2015). Numerical study of optimization of interference effect on pentagonal plan shaped tall building. *Asian Journal of Civil Engineering, 16*(8), 1123-1153.

[13]. Kar, R., & Dalui, S. K. (2016). Wind interference effect on an octagonal plan shaped tall building due to square plan shaped tall buildings. *International Journal of Advanced Structural Engineering (IJASE), 8*(1), 73-86.

[14]. Revuz, J., Hargreaves, D. M., & Owen, J. S. (2012). On the domain size for the steady-state CFD modelling of a tall building. *Wind and structures, 15*(4), 313-329.